© Med Sci Monit, 2009; 15(9): MT121-125
PMID: 19721407

Received: 2008.09.16
Accepted: 2009.01.11
Published: 2009.09.01

Authors' Contribution:
A Study Design
B Data Collection
C Statistical Analysis
D Data Interpretation
E Manuscript Preparation
F Literature Search
G Funds Collection

Ex-vivo detection of neural events using THz BioMEMS

Abdennour Abbas[1,2 ABCDEF], Thomas Dargent[1 AB], Dominique Croix[2 ACDEF], Michel Salzet[2 CDFG], Bertrand Bocquet[1 ABCEFG]

[1] Institute of Electronic, Microelectronic, and Nanotechnology, BioMEMS Group, UMR-CNRS 8520, University of Lille, Lille, France
[2] Annelids Neuroimmunology Laboratory, Leech Neuroregeneration Team, FRE CNRS 2933, University of Lille, Lille, France

Source of support: This work is supported by the University Interdisciplinary Program (PPF 2006 1803)

Summary

Background: Electromagnetic frequencies up to a few terahertz (THz) can yield real-time and noninvasive measurements on biological matter. Unfortunately, strong absorption in aqueous solutions and low spatial resolution return difficult free-space investigations. A new approach based on integrated THz circuits was used. The authors designed and fabricated a BioMEMS (Biological MicroElectro-Mechanical System) compatible with microfluidic circulation and electromagnetic propagation. It is dedicated to the *ex vivo* detection of nitric oxide synthase (NOS) activity, which is involved in neurodegenerative phenomena.

Material/Methods: The biological model was a leech's central nervous system. After its injury, the production of NO was observed and measured in the far-THz spectral domain. The nerve cord was put inside a BioMEMS realized in polydimethylsiloxane (PDMS) sealed on a glass wafer. Glass is a good material for supporting high-frequency integrated waveguides such as coplanar waveguides (CPWs). Measurements were performed with vectorial network analyser (VNA).

Results: The transmission parameter in the frequency range of 0.14–0.22 THz was measured through CPWs located just below the microchannel containing the injured leech nerve cord. The lesion caused a decreased transmission coefficient due to the NOS activity. L-NAME was injected inside the microchannel and it was verified that it inhibits this activity.

Conclusions: It was demonstrated that THz spectroscopy can detect a biochemical event, such as NOS activity around an injured leech's nerve cord, in real time. Future studies will be dedicated to quantitative measurements of the reaction products using the sophisticated management of several drugs allowed with microfluidic microsystems.

key words: **nitric oxyde • nitric oxyde synthase • Hirudo medicinalis • central nervous system • terahertz radiation • biological microelectrical-mechanical systems**

Full-text PDF: http://www.medscimonit.com/fulltxt.php?ICID=878163
Word count: 1924
Tables: –
Figures: 5
References: 21

Author's address: Bertrand Bocquet, IEMN, University of Lille, BP 60069, 59552 Villeneuve d'Ascq, France, e-mail: bertrand.bocquet@univ-lille1.fr

BACKGROUND

Today the emergence of microtechnology combined with microelectronic processes allows the creation of very sophisticated miniaturized objects for biological analysis. In these integrated circuits, called BioMEMS, we can mix electronic and microfluidic functions. The large majority of biosensors use the electrochemical principle or optical detection, but these techniques present some disadvantages, the principal one probably being the alteration of the biological activity by chemical reaction or by fluorescent tags bonded on molecules [1]. Microwaves up to the several ten gigahertz (GHz) and terahertz (THz) region between 0.1 to 10 THz could present a very interesting alternative in terms of free-label investigation [1,2] and more selective detection of radicals or biomolecules [3,4]. This spectrum could also provide additional information in molecular biology, for example the conformational states of proteins [5,6]. The results are expressed in terms of dielectric spectroscopy. Alternatively, an approach in the far-THz field is less attractive due to the poor spatial resolution of the wavelength. The use of planar waveguides inside integrated circuits makes possible these measurements.

Here, we wanted to detect nitric oxide synthase (NOS) activity in the leech nerve cord after injury. This study is of great interest due to the critical role of nitric oxide (NO), a gaseous molecule produced by NOS activity, in several biochemical networks, especially in the enhancement of nerve cord repair [7]. Today the detection of NOS activity is performed by histochemical staining, which requires fluorescent tags, whereas the monitoring of NO generation is generally realized by amperometric measurements [8]. However, these techniques remain difficult and depend strongly on the measurement conditions, such as the distance between the probe and the nerve cord, molecular diffusion phenomena, and the short half-life of NO in aqueous media (~6 s). The idea here was to immobilize a nerve cord inside a THz microfluidic system (Figure 1A). We have validated this approach using a mixed technology, such as polymer on silicon, for the analysis of protein solutions [9] and living cells [10,11]. The present study is dedicated to investigations of neural tissues investigations.

MATERIAL AND METHODS

Animal model

Our biological model was the leech *Hirudo medicinalis*, which is a very interesting and largely studied invertebrate. A lesion or a cut of its nerve cord, which represents the central nervous system (CNS), causes biochemical events leading to complete neuron regeneration and restoration of biological function in approximately four weeks after damage [12]. Note that synapse regeneration in mammals is successful in the peripheral nervous system (PNS), but fails very quickly in the CNS [13]. After nerve cord injury, the rapid production of NO is one of the early events occurring at the lesion [14]. This production is catalyzed by an isoenzyme family called NO synthases (NOS, EC. 1.14.13.39), according to the reaction: L-arginine + 2 NADPH + 2 O_2 + 2 H^+ → NO + L-citrulline + 2 $NADP^+$ + 2 H_2O (NADPH: nicotinamide adenine dinucleotide phosphate). Moreover, treatment with the NOS inhibitor L-N^G-nitroarginine methylester (L-NAME) blocks the repair mechanism, showing the important role of NOS in the modulation of axon growth [7,15]. However, the application of exogenous NO with the NO donor Spermine NONOate (SPNO) increases the concentration and leads to a total blocking of regeneration. In mammals under pathological circumstances, the significant increase in NOS activity induces toxicity and/or neuron apoptosis [16]. The produced NO is involved in neurodegenerative phenomena, particularly Alzheimer's diseases and Parkinsonism [17]. An important question is how the precise regulation of NOS activity in the leech induces neuron regeneration and not cell death. Real-time monitoring of NOS activity is a major step towards understanding the role of NO in nerve repair and how man loses his capacity to regenerate his CNS during neurodegenerative disorders.

BioMEMS design

Before designing our microsystem, the average dimensions of the connectives and ganglions of the leech *Hirudo medicinalis* were determined. The microchannel (width: 450 µm, depth: 1 mm, length: 4 cm, volume: <15 µl) is matched to the nerve cord dimensions to improve its immobilization and limit the medium's evaporation. The THz BioMEMS design uses a classical technology based on PDMS due to the large dimensions of the microchannel [18]. The PDMS is prepared by mixing the precursor Sylgard 184 (Dow Corning) with the cross-linking agent at a 10:1 weight ratio. We use a coplanar waveguide (CPW) which is well suited to this measurement [19]. It is placed under the probes of the vectorial network analyzer (VNA) (Figure 1B). This planar waveguide is composed of three conductors and designed on a glass substrate (Figure 2A). The latter has low losses in THz propagation and its transparency allows further use of contrast phase microscopy for the observation of the nerve cord under measurement. We optimized the propagation condition on a real microsystem composed of a tank filled with liquid water. Many geometric configurations in terms of the slot width to central conductor width ratio are possible to obtain the desired impedance of 50 Ω, which is recommended for connection to the VNA. Simulations were performed with full 3D software called Microwave Studio® from Computer Simulation Technology (CST) and based on a finite element method (FEM). The true sizes take into account the propagation of the fundamental non-dispersive mode and a small excursion of the electric field for reducing the radiated losses. An example of a simulated structure is shown on the Figure 2B. We obtained a good correlation between the computed and the measured values on water (Figure 3).

The microsystem is realized on a 2-inch-square glass substrate. A thin binding of a 200-Å chromium (Cr) layer was sputtered onto the substrate before the deposition of a 0.5-µm gold (Au) layer. Then both the gold and chromium are etched to create the CPW lines. Two-step photolithography was adopted for the substrate processing. The PDMS channel was obtained by molding in a mechanically etched piece of Teflon®. To obtain a permanent bond of the device, both the glass substrate and the PDMS channel were exposed separately to plasma oxidation before joining them together.

Spectral measurements

The nerve chains were extracted from adult leeches weighing from 2 to 3 mg and maintained in Ringer's solution (pH

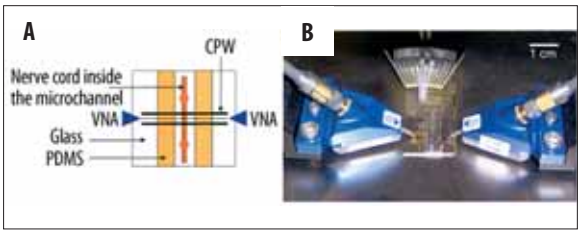

Figure 1. (**A**) Top view of immobilized nerve cord in the microchannel probed orthogonally by the VNA. (**B**) Photo of the BioMEMS (rectangular transparent structure) positioned between two VNA probes (in blue).

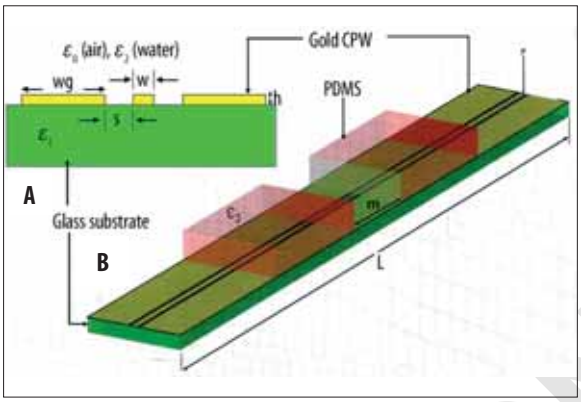

Figure 2. Simulated structure. (**A**) Cross section of the CPW: w_g=300 µm, w=48 µm, s=10 µm, h=0.5 µm, ε_0=1, and ε_1=4.82 with tan δ_1=0.0054; ε_2 is defined by the 2nd order Debye model (ε_{static}=77.97, ε_∞=4.59, relaxation time =8.32 ps). (**B**) 3D view of the cross-section of the microsystem with two walls of 3 mm PDMS, m (microchannel width) =450 µm, L (CPW length) =11 mm, ε_3=2.68 with tan δ_3=0.11.

7.4) for their survival. They were manually placed and immobilized inside the open microchannel after PDMS-glass bonding. Dissection and lesions performed during the experiment were carried out under aseptic conditions using Patscheff scissors. L-NAME hydrochloride was purchased from Cayman Chemical. Solutions with different concentrations were prepared by dissolving L-NAME powder in Ringer's solution and injections were performed using a 33-gauge Hamilton syringe (internal diameter: 0.21 mm) obtained from Hamilton Bio. The transmission measurements were carried out at room temperature under aerobic conditions. The VNA is an Anritsu 37147C associated with mixers of reference V05VNA2-T/R from OML (Oleson Microwave Laboratories) working in a bandwidth of 0.14-0.22 THz. We use line-reflect-match (LRM) calibration with a calibration kit (reference 101–190B of Cascade Microtech). The analyzer is gauged in the plane of the measurement probes. Here we exploited only the transmission modulus relative to the wave absorption.

Results

To study the transmission spectral characteristics of the CPW, we initially carried out tests separately on well-known deionized water and on Ringer's solution (115 mM NaCl, 4 mM KCl_2, and 1.8 mM $CaCl_2$), buffered at pH 7.4 with 10 mM

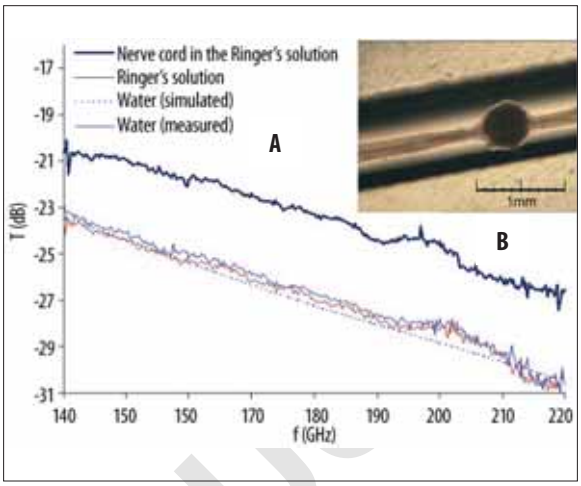

Figure 3. (**A**) Transmission curves of deionized water, Ringer's solution, and nerve cord in the Ringer's solution. Simulated (dashed blue line) and experimental (solid blue line) transmission of the CPW on the water show good correlation between the measured and the computed values. (**B**) The nerve cord, composed of ganglions (dark disk) and connectives, is lightly stretched inside the PDMS microchannel.

Tris maleate (Figure 3A). As can be seen from the computed values obtained for pure water, the transmission coefficient decreases with increasing frequency, but remains valuable for a good measurement. The very small volume matches our measurements well despite the high water absorption. Note that we can observe some small rebound phenomena due to the standing waves minimized by the impedance optimization. The same figure shows a very small difference between the spectral responses of water and Ringer's solution, which can be explained by the fact that moderate ionic concentrations have negligible effects on transmission spectra [20]. The measured values were stables and reproducible and the measurement errors are estimated at ±0.1 dB. This result shows that Ringer's solution can be a useful survey medium for *in vivo/ex vivo* studies by THz spectroscopy. Therefore, when the nerve cord was immobilized inside the microchannel containing Ringer's solution, we observed an improvement in the transmission coefficient (Figure 3A,B). This is mainly due to the displacement of water by nerve tissues.

The second step was the calibration with L-NAME in the millimolar concentration range. Figure 4 shows that Beer's law is validated for the millimolar concentration in the frequency range of 0.14–0.20 GHz. We can clearly see a linear change in THz transmission with the concentration of L-NAME. The increase in transmission in this case can be explained by the increasing number of bound water molecules (hydration shell) that present low mobility and consequently lower dielectric constant than free water [21].

Discussion

In these experiments, the detection limit of the BioMEMS reached down to 0.01 g/ml. This limit, obtained by varying L-NAME concentrations, concerns only hydrated biomolecules that increase transmission and not the NOS activity

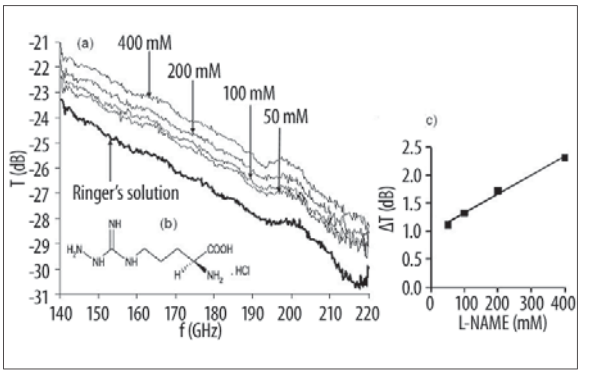

Figure 4. (a) Transmission curves obtained at various concentrations of solvated L-NAME in Ringer's solution. (b) Semi-developed chemical formula of L-NAME. (c) Linear change in THZ transmission with the concentration of L-NAME. ΔT is obtained by the average values of the subtraction of the waveguide transmission in the presence of Ringer's solution ($\Delta T = T_{total} - T_{Ringer}$) for each frequency in the range 0.14–0.20 THz.

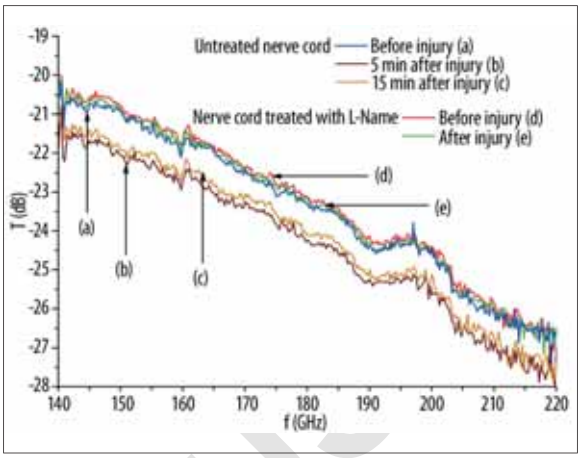

Figure 5. Transmission curves obtained with nerve cords under different conditions in the Ringer's solution. An injury of the nerve cord producing NO and L-citruline creates a change of 0.8 dB (b) and (c) compared with the reference signal obtained with an intact cord (a). The reproducibility of these measurements was validated on six different cords. L-NAME is used here to block NO production after injury. There is no significant change in the transmission curves of the nerve cords treated with L-NAME before (d) and after injury (e), indicating that change in THZ transmission is due mainly to NO and/or L-citruline released by the nerve cord after the lesion.

products (probably NO) that increase absorption, as we can see below. The last step of these experiments was a preliminary comparative study of the leech nerve cord before and after injury. The aim was to block NOS activity after injury and observe the change in THz transmission features. First the nerve cords were injured directly inside the microchannel filled with Ringer's solution without any treatment (Figure 5). As can be seen, the lesion caused a decreased transmission coefficient from approximately 0.8±0.1 dB compared with the intact cord. Curves 5(b) and (c) show, respectively, that after injury, NOS activity immediately reached a peak of intensity and then decreased over time, never returning to the pre-injury level. Secondly, nerve cords were exposed to 1 mM L-NAME for 40 min before injury. L-NAME is the antagonist of L-arginine amino acid. Thus it inhibits the NO synthase enzyme and then blocks NO and L-citruline production. Here, L-NAME was used as a reference sample, and no statistically significant differences in the transmission of the intact nerve cord and the injured nerve cord were observed after L-NAME treatment. Similar results obtained by the amperometric method are described in the literature [14]. Note that the L-NAME concentration of 1 mM had no effect on the transmission features according to the limited sensitivity of the present BioMEMS. The transmission change described above is likely due to the highest absorbance of THz radiation by the released products.

Conclusions

Studies of the interaction between THz radiation and reactive molecules in liquid phase would lead to a better understanding of the biological activity. This study demonstrates that the combination of THz and microfluidic circuits inside a BioMEMS allows us to perform *ex vivo* measurements. The main interest is the integration on a micrometric scale to obtain fine spatial resolution and selective detection. The second advantage is the very small volume, which leads to a huge increase in the local concentration of the reaction products. We specifically designed a microsystem for *ex vivo* analysis of leech nerve cords and the preliminary results show two main considerations: Firstly, our measurements show clearly that it is possible to use THz spectroscopy for the detection of biochemical reaction in aqueous solution. Secondly, we characterized the NOS activity around a leech nerve cord. Future experimental tests will be dedicated to the investigation of analytical parameters (sensitivity, detection limits) and the time monitoring of NOS activity. We will obtain quantitative measurements of the reaction products by using the sophisticated management of several drugs allowed with microfluidic microsystems. These studies will improve our knowledge of the NO production process, and then of nerve repair mechanisms.

References:

1. Facer GR, Notterman DA, Sohn LL: Dielectric spectroscopy for bioanalysis: From 40 Hz to 26.5 GHz in a microfabricated wave guide. Appl Phys Lett, 2001; 78: 996–98
2. Hefti J, Pan A, Kumar A: Sensitive detection method of dielectric dispersions in aqueous-based, surface-bound macromolecular structures using microwave spectroscopy. Appl Phys Lett, 1999; 75: 1802–4
3. Smye SW, Chamberlain JM, Fitzgerald A, Berry E: The interaction between TeraHertz radiation and biological tissue. Phys Med Biol, 2001; 46: 101–12
4. Siegel PH: Terahertz technology in biology and medicine. IEEE-TMTT, 2004; 52: 2438–47
5. Globus T, Khromova T, Lobo R et al: THz characterization of lysozyme at different conformations. Proc of SPIE, 2005; 5790: 54–65
6. Markelz AG, Whitmire S, Hillebrecht J, Birge R: THz time domain spectroscopy of biomolecular conformational modes. Phys Med Biol, 2002; 47: 3797–805
7. Chen AS Kumar M, Sahley CL, Muller KJ: Nitric Oxide Influences Injury-Induced Microglial Migration and Accumulation in the Leech CNS. J Neurosci, 2000; 20: 1036–43
8. Amatore C: Monitoring in Real Time with a Microelectrode the Release of Reactive Oxygen and NitrogenSpecies by a Single Macrophage Stimulated by its Membrane Mechanical Depolarization. ChemBioChem, 2006; 7: 653–61

9. Mille V, Bourzgui NE, Vivien C et al: New technology for high throughput THz BioMEMS Proc. of the 28th IEEE-EMBS Int. Conf. (New York, USA), 2006; 3505–8
10. Treizebré A, Akalin T, Bocquet B: Planar excitation of Goubau transmission lines for THz BioMEMS IEEE-MWCL, 2005; 15: 886–88
11. Treizebré A, Bocquet B: Nanometric metal wire as a guide for THz investigation of living cells. Int J Nanotechnol, 2008; 6/7/8: 784–95
12. Modney BK, Sahley CL, Muller KJ: Regeneration of a Central Synapse Restores Nonassociative Learning. J Neurosci, 1997; 17: 6478–82
13. Fawcett J: Astrocytic and neuronal factors affecting axon regeneration in the damaged central nervous system Cell Tissue Res, 1997; 290: 371–77
14. Kumar SM, Porterfield DM, Muller KJ et al: Nerve Injury Induces a Rapid Efflux of Nitric Oxide (NO) Detected with a Novel NO. Microsensor J Neurosci, 2001; 21: 215–20
15. Shafer OT, Chen A, Kumar SM et al: Injury-induced expression of endothelial nitric oxide synthase by glial and microglial cells in the leech central nervous system within minutes after injury. Proc R Soc Lond, 1998; B265: 2171–75
16. Bonfoco E, Krainc D, Nicotera P, Lipton SA: Apoptosis and necrosis: Two distinct events induced, respectively, by mild and intense insults with N-methyl-D-aspartate or nitric oxide/superoxide in cortical cell cultures. Proc Natl Acad Sci USA Neurobiology, 1995; 92: 7162–66
17. Zhang L, Valina L, Dawson TM: Role of nitric oxide in Parkinson's disease. Pharmacology & Therapeutics, 2006; 109: 33–41
18. McDonald JC, Duffy DC, Anderson JR et al: Fabrication of microfluidic systems in poly(dimethylsiloxane). Electrophoresis. 2000; 21: 27–40
19. Gupta KC, Garg R, Bahl I, Bhartia P: Microstrip Lines and Slotlines. 2nd edition. Artech House (Boston), 1996
20. Xu J, Plaxco KW, Allen SJ et al: 0.15–3.72 THz absorption of aqueous salts and saline solutions. Appl Phys Lett, 2007; 90: 031908–10
21. Mickana SP, Dordickc J, Munchd J et al: Terahertz spectroscopy of bound water in nano suspensions Proc. of SPIE 2002;4937: 49–61